

HINT: A Toolbox for Hierarchical Modeling of Neuroimaging Data

Joshua Lukemire, Yikai Wang, Amit Verma, and Ying Guo
Emory University

Abstract

The modular behavior of the human brain is commonly investigated using independent component analysis (ICA) to identify spatially or temporally distinct functional networks. Investigators are commonly interested not only in the networks themselves, but in how the networks differ in the presence of clinical or demographic covariates. To date, group ICA methods do not directly incorporate these effects during the ICA decomposition. Instead, two-stage approaches are used to attempt to identify covariate effects (Calhoun et al. (2001); Beckmann et al. (2009)). Recently, Shi and Guo (2016) proposed a novel hierarchical covariate-adjusted ICA (hc-ICA) approach, which directly incorporates covariate information in the ICA decomposition, providing a statistical framework for estimating covariate effects and testing them for significance. In this work we introduce the Hierarchical Independent Component Analysis Toolbox, HINT, to implement hc-ICA and other hierarchical ICA techniques.

1 Introduction

In recent years, there has been a growing interest in network based approaches to describing brain function. Under a network approach, observed brain signals represent a combination of signals generated from distinct brain functional networks. For example, in functional magnetic resonance imaging (fMRI), the observed blood-oxygen-level-dependent (BOLD) signal can be viewed as a combination of contributions from different brain networks. These brain functional networks can potentially aid in understanding the large scale functional structure of the brain as they have been shown to be present across a wide variety of subjects and across a range of different experimental conditions (Smith et al., 2013). Consequently, studying these brain functional networks has become a topic of great interest. The most popular brain network estimation tool is independent component analysis (ICA), which identifies brain functional networks as latent source signals that are close to statistically independent.

Some of the earliest applications of ICA to the study of brain networks were to single subject fMRI data. Spatial ICA (McKeown et al., 1997), which separates the observed data into independent spatial maps and corresponding time courses is the most popular technique. For fMRI data with a large number of measurements, it is also possible to perform temporal ICA (Smith et al., 2012), which separates the observed data into temporally coherent maps.

While methods for single subject ICA are quite well established, the application of ICA to multiple subjects or groups is still an area of active development. Existing techniques for group level ICA are frequently based on temporal-concatenation group ICA (tc-gICA), which assumes that brain functional networks have the same spatial pattern across different subjects. Under a tc-gICA approach, the timepoints of the subject level data are stacked and the spatial source signals (ICs) are extracted. The subject level ICs are then recovered using techniques such as back-reconstruction (Calhoun et al., 2001) or dual-regression (Beckmann et al., 2009). Inference

on covariate effects under these frameworks requires secondary hypothesis testing, which fails to take into account the random variation from the reconstruction of the subject level data.

Recently, Shi and Guo (2016) proposed a hierarchical covariate adjusted independent component analysis (hc-ICA) technique for estimating independent components in brain imaging data in the presence of covariates. This novel technique is fundamentally different from other methods allowing comparison of groups within an ICA framework, as it directly accounts for covariate patterns in the estimation stage. Additionally, it has the desirable properties of providing model based interpretation of sub-population results and a statistical framework for testing covariate effects. For example, in their work, Shi and Guo (2016) showed that hc-ICA could find significant differences in a task network between women with and without post traumatic stress disorder even after FDR correction, whereas dual regression could not.

In this work we introduce the Hierarchical INdependent component analysis Toolbox (HINT), a Matlab toolbox that serves as a platform for hierarchical ICA techniques. At this time, the toolbox implements the hc-ICA technique of Shi and Guo (2016), with further extensions of this approach, including a longitudinal ICA method, in active development. The intent of this toolbox is to provide neuroimaging researchers with an easy-to-use tool for utilizing hierarchical ICA techniques on fMRI data, allowing them to estimate the brain networks of interest and to test hypothesis about covariate effects.

The HINT allows the user to input their data, perform the preprocessing required by the hc-ICA approach, obtain initial guesses for the model parameters, and remove noise ICs or ICs that are not of interest from the analysis. Estimation within the HINT is carried out via an Expectation Maximization (EM) algorithm as described in Section 2.3. After obtaining parameter estimates, the toolbox provides the user with the ability to visualize the estimated ICs and perform model-based hypothesis testing of the covariate effects and linear combinations of the covariate effects.

In what is to follow, we review the hc-ICA model in Section 2. We also describe our EM algorithm and introduce our model-based variance-covariance estimator for the covariate effects. Then, in Section 3, we provide a walkthrough of the toolbox features, explaining how they interface with the statistical model. Finally, in Section 4 we discuss future directions for HINT and provide some concluding remarks.

2 The hc-ICA Model

2.1 Preprocessing

Before the hc-ICA model parameters can be estimated, the subject level data must first be preprocessed as described in Shi and Guo (2016). For number of time points T and number of voxels V , each subject's $T \times V$ data are prewhitened to be $q \times V$ as:

$$\mathbf{Y}_i = (\mathbf{\Lambda}_{i,q} - \sigma_{i,q}^2 \mathbf{I}_q)^{-1/2} \mathbf{U}_{i,q}^T \tilde{\mathbf{Y}}_i, \quad (1)$$

where q is the number of independent components, $\mathbf{\Lambda}_{i,q}$ contains the first q eigenvalues and $\mathbf{U}_{i,q}$ contains the first q eigenvectors as obtained by a singular value decomposition of the original data $\tilde{\mathbf{Y}}_i$. The residual variance, $\sigma_{i,q}^2$, is taken to be the average of the $T - q$ smallest eigenvalues. To perform this preprocessing, the user must input the number of principal components and the number of independent components, which can be determined using the Laplace approximation method (Minka, 2001).

2.2 Modeling

The hc-ICA model consists of two levels: a subject level and a group level. At the first level, each subject's preprocessed data is decomposed into a linear mixture of subject-level independent components (ICs) as

$$\mathbf{y}_i(v) = \mathbf{A}_i \mathbf{s}_i(v) + \mathbf{e}_i(v), \quad (2)$$

where $\mathbf{s}_i(v) = [s_{i1}(v), s_{i2}(v), \dots, s_{iq}(v)]^T$ is a $q \times 1$ vector, and each $s_{il}(v)$ contains the spatial source signal of the l th IC at the v th voxel for subject i . \mathbf{A}_i is the $q \times q$ orthogonal mixing matrix for subject i , which mixes with the spatial source signals to generate the observed data. We assume that the $q \times 1$ noise vector $\mathbf{e}_i(v) \sim N(\mathbf{0}, \mathbf{E}_v)$. We can assume that this term is independent across voxels, as the spatial source signals will model any spatial correlation that is present among the voxels (Hyvärinen and Oja, 2000; Guo and Pagnoni, 2008). Moreover, by prewhitening the data as described in Section 2.1, we remove the temporal autocorrelation, therefore we can assume that the noise covariance is identical across voxels and is isotropic (Beckmann et al., 2005; Guo, 2011), i.e. $\mathbf{E}_v = \sigma_0^2 \mathbf{I}_q$.

The subject level ICs are modeled as a combination of population-level spatial source signals, covariate effects, and subject-specific random variabilities according to:

$$\mathbf{s}_i(v) = \mathbf{s}_0(v) + \beta(v)^T \mathbf{x}_i + \gamma_i(v), \quad (3)$$

where $\mathbf{s}_0(v) = [s_{01}(v), s_{02}(v), \dots, s_{0q}(v)]^T$ contains population level source signals for each of the q ICs. The covariate information is encoded in $\mathbf{x}_i = [x_{i1}(v), x_{i2}(v), \dots, x_{ip}(v)]^T$, a $p \times 1$ vector with the covariate settings for subject i . The $q \times 1$ error vector $\gamma_i(v)$ reflects the random variability between subjects that is leftover after controlling for the covariate effects. Thus, each subject level IC can be viewed as a baseline component common across the entire population that is modified by covariate effects. We assume that $\gamma_i(v) \sim N(\mathbf{0}, \mathbf{D})$, where $\mathbf{D} = \text{diag}(\nu_1^2, \dots, \nu_q^2)$. We allow the variances to be IC-specific to allow for different levels of between-subject random variability.

The population level spatial source signals, $\mathbf{s}_0(v)$, are modeled under a mixtures of Gaussians (MoG) approach (Guo, 2011; Guo and Tang, 2013). That is, for IC l , $l = 1, \dots, q$, we have:

$$s_{0l}(v) \sim \text{MoG}(\boldsymbol{\pi}_l, \boldsymbol{\mu}_l, \sigma_l^2), \quad (4)$$

for $v = 1, \dots, V$, where $\boldsymbol{\pi}_l = [\pi_{l1}, \pi_{l2}, \dots, \pi_{lm}]^T$ denotes the vector of probabilities of belonging to each component. The number of components, m , is taken to be 3. Under this setup, one component is reserved for background fluctuation, one for positive BOLD effects, and one for negative BOLD effects (Beckmann and Smith, 2004).

We use latent state variables to track the contribution of each IC to the signal at a voxel (McLachlan and Peel, 2004). We define $\mathbf{z}(v) = [z_1(v), z_2(v), \dots, z_q(v)]^T$ as the latent state variable. Each element of $\mathbf{z}(v)$ corresponds to the MoG contribution from IC l , $l = 1, \dots, q$. That is, for a given element l of $\mathbf{z}(v)$ and for $m = 3$, $P(z_l(v)) = j = \pi_l$. Thus there are m^q possible unique vectors $\mathbf{z}(v)$.

2.3 EM Algorithms

Under the hierarchical framework implemented in HINT, parameter estimates are obtained using an EM algorithm to maximize the complete data log-likelihood. As derived in Shi and Guo (2016), the expectation of the complete data log-likelihood can be written:

$$Q(\boldsymbol{\Theta} | \hat{\boldsymbol{\Theta}}^{(k)}) = \sum_{v=1}^V E_{\mathbf{s}(v), \mathbf{z}(v) | \mathbf{y}(v)} [l_v(\boldsymbol{\Theta}; \mathcal{Y}, \mathcal{X}, \mathcal{S}, \mathcal{Z})], \quad (5)$$

where $\mathcal{Y} = \{\mathbf{y}_i(v) : i = 1, \dots, N, v = 1, \dots, V\}$, $\mathcal{X} = \{\mathbf{x}_i(v) : i = 1, \dots, N\}$, $\mathcal{S} = \{\mathbf{s}_i(v) : i = 1, \dots, N, v = 1, \dots, V\}$, and $\mathcal{Z} = \{\mathbf{z}(v) : v = 1, \dots, V\}$. The model parameters are $\Theta = \{\{\beta(v)\}, \{\mathbf{A}_i\}, \mathbf{E}, \mathbf{D}, \{\pi_l\}, \{\mu_l\}, \{\sigma_l^2\} : i = 1, \dots, N, v = 1, \dots, V, l = 1, \dots, m\}$.

The primary driver of computation time for the hc-ICA algorithm is the cardinality of $\mathbf{z}(v)$, the latent state variables. An exact EM algorithm would have to consider all m^q possible $\mathbf{z}(v)$, a number of combinations which will quickly spiral out of control as the number of ICs increases. This leads us to implement an approximate EM algorithm which considers only a sub-space of the latent state vector. More specifically, the approximate EM algorithm considers only the $\mathbf{z}(v)$ in which at most one element does not correspond to background fluctuation. Thus this approximate EM algorithm only grows linearly in the number of ICs.

This approximation is motivated by the fMRI literature, which holds that spatial signals in the brain are sparse (Daubechies et al., 2009). That is, in a given brain functional network, most of the voxels are exhibiting only background fluctuation, and only a small proportion of voxels will be activated by the network (Biswal and Ulmer, 1999). This implies that there should not be much overlap of independent spatial components; if a voxel is a member of one IC it is likely not a member of any other ICs. Thus it is reasonable to consider latent state vectors $\mathbf{z}(v)$ in which at most one component does not belong to background noise. That is, vectors in which only one element of $\mathbf{z}(v) \neq 1$. Shi and Guo (2016) present a proof that this subspace approximation is valid. The procedure for the Approximate EM algorithm is presented in Algorithm 1.

Algorithm 1: The approximate EM algorithm, which is based on the subspace $\tilde{\mathcal{Z}}$

Initial Values: Starting values of $\hat{\Theta}^{(0)}$ and $\hat{\beta}^0$ obtained using estimates from the GIFT

while *iteration* < *max iterations* and $\frac{\|\hat{\Theta}^{(k+1)} - \hat{\Theta}^{(k)}\|}{\|\hat{\Theta}^{(k)}\|} > \epsilon$ **do**

E Step:

1. Determine $\tilde{p}[\mathbf{s}(v)|\mathbf{y}(v); \hat{\Theta}^{(k)}]$ and the corresponding marginal probabilities as:

- (a) Evaluate the multivariate Gaussian $p[\mathbf{s}(v)|\mathbf{z}(v), \mathbf{y}(v); \hat{\Theta}^{(k)}]$
 - (b) Evaluate $\tilde{p}[\mathbf{z}(v)|\mathbf{y}(v); \hat{\Theta}^{(k)}]$ on the subset $\tilde{\mathcal{Z}}$
 - (c) Combine the above steps to obtain
- $$\tilde{p}[\mathbf{s}(v), \mathbf{z}(v)|\mathbf{y}(v); \hat{\Theta}^{(k)}] = p[\mathbf{s}(v)|\mathbf{z}(v), \mathbf{y}(v); \hat{\Theta}^{(k)}] \times \tilde{p}[\mathbf{z}(v)|\mathbf{y}(v); \hat{\Theta}^{(k)}]$$

Leading to the marginal $\tilde{p}[\mathbf{s}(v)|\mathbf{y}(v); \hat{\Theta}^{(k)}] = \sum_{\mathbf{z}(v) \in \tilde{\mathcal{Z}}} \tilde{p}[\mathbf{s}(v), \mathbf{z}(v)|\mathbf{y}(v); \hat{\Theta}^{(k)}]$

2. Evaluate the conditional expectations in $Q(\Theta|\hat{\Theta}^{(k)})$ with regard to $\tilde{p}[\mathbf{s}(v), \mathbf{z}(v)|\mathbf{y}(v); \hat{\Theta}^{(k)}]$

M Step:

- 1. Update $\beta(v)$, \mathbf{A}_i , π_{lj} , σ_{lj}^2 , replacing the exact conditional moments with their counterparts based on $\tilde{p}[\mathbf{s}(v)|\mathbf{y}(v); \hat{\Theta}^{(k)}]$.
- 2. Update the variance parameters \mathbf{D} and \mathbf{E} , replacing the exact conditional moments with their counterparts based on $\tilde{p}[\mathbf{s}(v)|\mathbf{y}(v); \hat{\Theta}^{(k)}]$

end

Even using the subspace-based approximation these methods can be quite time consuming, as there are a very large number of parameters to update with each EM iteration. We have taken steps to ensure that the computation time is as fast as possible. Importantly, we have used vectorization within the Matlab environment in order to reduce computation time. One

Matlab library, MTIMESX (Tursa, 2011), has featured prominently here, as well as in-built Matlab functions for handling vector operations such as bsxfun.

2.4 Inference for covariate effects

In this section, we propose a statistical inference procedure for testing covariate effects in the HINT framework. Typically maximum likelihood inference is based on asymptotic properties of the estimator, and the inverse of the information matrix is used as the asymptotic variance-covariance matrix. However, under the hc-ICA model the dimension of the parameter space is ultra-high and the information matrix is not sparse. Therefore, we cannot estimate the invert of information matrix. To address this issue, following Shi and Guo (2016) we propose an estimator of the empirical variance-covariance matrix of the covariate effects at each voxel by connecting the hc-ICA model to standard multivariate linear models.

We first rewrite the hc-ICA model in the following form:

$$\mathbf{A}'_i \mathbf{y}_i(v) = \boldsymbol{\mu}_{\mathbf{z}(v)} + \mathbf{X}_i \mathbf{b}(v) + \boldsymbol{\psi}_{\mathbf{z}(v)} + \boldsymbol{\gamma}_i(v) + \mathbf{A}'_i \mathbf{e}_i(v), \quad (6)$$

where $\mathbf{b}(v) = \text{vec}[\boldsymbol{\beta}(v)']$ and $\mathbf{X}_i = \mathbf{x}'_i \otimes \mathbf{I}_q$. This model (6) can be further re-expressed as

$$\mathbf{y}^*_i(v) = \mathbf{X}^*_i \mathbf{b}^*(v) + \boldsymbol{\zeta}_i(v). \quad (7)$$

where $\mathbf{y}^*_i(v) = \mathbf{A}'_i \mathbf{y}_i(v)$, $\mathbf{X}^*_i = [\mathbf{I}_q, \mathbf{X}_i]$, $\mathbf{b}^*(v) = [\boldsymbol{\mu}'_{\mathbf{z}(v)}, \mathbf{b}(v)']'$ and $\boldsymbol{\zeta}_i(v) = \boldsymbol{\psi}_{\mathbf{z}(v)} + \boldsymbol{\gamma}_i(v) + \mathbf{A}'_i \mathbf{e}_i(v) \sim N(\mathbf{0}, \mathbf{W}_i(v))$ is the multivariate zero-mean Gaussian noise term where $\mathbf{W}_i(v) = \boldsymbol{\Sigma}_{\mathbf{z}(v)} + \mathbf{A}_i \mathbf{E}_v \mathbf{A}'_i + \mathbf{D}$. Because the mixing matrix \mathbf{A}_i is orthogonal, the first level residual has identical and isotropic variance term $\mathbf{E}_v = \sigma_0^2 \mathbf{I}$, and we have the same variance covariance term $\mathbf{W}_i(v) = \mathbf{W}(v) = \boldsymbol{\Sigma}_{\mathbf{z}(v)} + \mathbf{D} + \sigma_0^2 \mathbf{I}_q$ for all subjects at a given voxel.

Conditioned on the latent state variable $\mathbf{z}(v)$, (7) can be viewed as a general multivariate linear model at each voxel. The major distinction of (7) from the standard linear model is that the dependent variable $\mathbf{y}^*(v)$ not only depends on the observed data $\mathbf{y}(v)$ but also involves unknown parameters \mathbf{A}_i . This leads us to propose the following variance estimator for $\hat{\mathbf{b}}^*(v)$:

$$\hat{\text{Var}}\{\hat{\mathbf{b}}^*(v)\} = \left(\sum_{i=1}^N \mathbf{X}^{*T}_i \mathbf{W}(v)^{-1} \mathbf{X}^*_i \right)^{-1}. \quad (8)$$

Calculation of $\hat{\mathbf{b}}^*(v)$ requires an estimate of $\mathbf{W}(v)$. We propose two estimators of $\mathbf{W}(v)$: a theoretical estimator based on the hc-ICA model and EM outputs and an empirical estimator based on linear regression theory. For the theoretical estimator, we note that based on the EM algorithm, the unknown parameters in $\mathbf{W}(v)$ can be estimated simultaneously. Therefore, we plug-in the estimated parameters into \mathbf{W} and have:

$$\hat{\mathbf{W}}(v)^{(Theo)} = \hat{\boldsymbol{\Sigma}}_{\mathbf{z}_{mode}(v)} + \hat{\mathbf{D}} + \hat{\sigma}_0^2 \mathbf{I}_q, \quad (9)$$

where $\mathbf{z}_{mode}(v)$ is the latent states with highest posterior probability $p(\mathbf{z}(v)|\mathbf{y}(v), \hat{\boldsymbol{\Theta}})$. On the other hand, the empirical estimator is set to be:

$$\hat{\mathbf{W}}(v)^{(Emp)} = \frac{1}{N} \sum_{i=1}^N \left(\hat{\mathbf{A}}'_i \mathbf{y}_i(v) - \hat{\boldsymbol{\mu}}_{\mathbf{z}_{mode}(v)} - \mathbf{X}_i \text{vec}[\hat{\boldsymbol{\beta}}(v)'] \right)^{\otimes 2}, \quad (10)$$

which can be more robust to violation of the model assumptions.

Plugging in the estimates of $\mathbf{W}(v)$ into (8), the variance estimator for $\hat{\mathbf{b}}^*(v)$ is $\text{Var}\{\hat{\mathbf{b}}^*(v)\} = \frac{1}{N} \left(\sum_{i=1}^N \mathbf{X}_i^{*T} \hat{\mathbf{W}}(v)^{-1} \mathbf{X}_i^* \right)^{-1}$.

Based on these results, hypothesis testing on any linear combination of the covariate effects can be conducted by estimating the corresponding z-statistics and the p -values. Specifically, we would like to test on some sub-population level map. For this case, hypothesis testing can be conducted by defining an appropriate contrast, \mathbf{c} , such that $\mathbf{c}^T \boldsymbol{\beta}$ gives the test of interest. For example, if β_1 corresponds to race and β_2 corresponds to sex, the hypothesis that the effect of race and sex are equal could be testing with the contrast matrix $\mathbf{c} = [1 \ -1]^T$. This hypothesis testing functionality is incorporated into the beta covariate display window as described in Section 3.3.

3 Functionality

An hc-ICA analysis via the HINT consists of the following steps: Data loading, preprocessing, obtaining an initial guess, estimation via EM algorithm, and testing hypothesis about covariate effects. The HINT partitions these steps into three panels:

1. The preprocessing panel, where the user inputs the data, selects the number of principal components and independent components, and obtains initial guesses for the EM algorithm.
2. The estimation panel, which allows the user to select the maximum number of iterations, and the convergence criteria. The user can then run the algorithm and monitor its progress using two change plots.
3. The display panel, which allows the user to view their results and compare sub-populations with different covariate values. This panel also allows for model-based inference. The user can test hypothesis about the covariates or linear combinations of the covariates.

3.1 Preprocessing Panel

3.1.1 The runinfo file

The hc-ICA analysis in the HINT is controlled using a file titled the “runinfo” file containing the objects listed in Table 1. It is automatically created when the user selects the “Save setup and continue” option displayed in Figure 1. This file can be referenced during subsequent uses of the toolbox to avoid repeating previous work. The runinfo file is a single file, and thus can be easily moved across different computers or networks. The filepaths within the runinfo file can easily be updated using the “prepare a script analysis” option provided in the “Tools” menu.

3.1.2 Data Input

The user has two options when inputting data for the analysis. They can start a new analysis by selecting “Import Nifti files” and inputting the required files. Alternatively, if the user wishes to continue an analysis that they have already started, they can load the runinfo file corresponding to that analysis using the “Load saved .mat data” option, allowing them to avoid re-performing preprocessing and initial guess estimation.

When starting a new analysis, the user is instructed to provide three elements: the nifti files containing the subject-level data, a mask file, and the covariate file. The covariate file must be a .csv file conforming to a specific structure. First, the top row of the file should contain column information. For the first column, this is the label “subject” and for subsequent columns this is the variable name. Then, each following row of the file should start with the filename for the subject

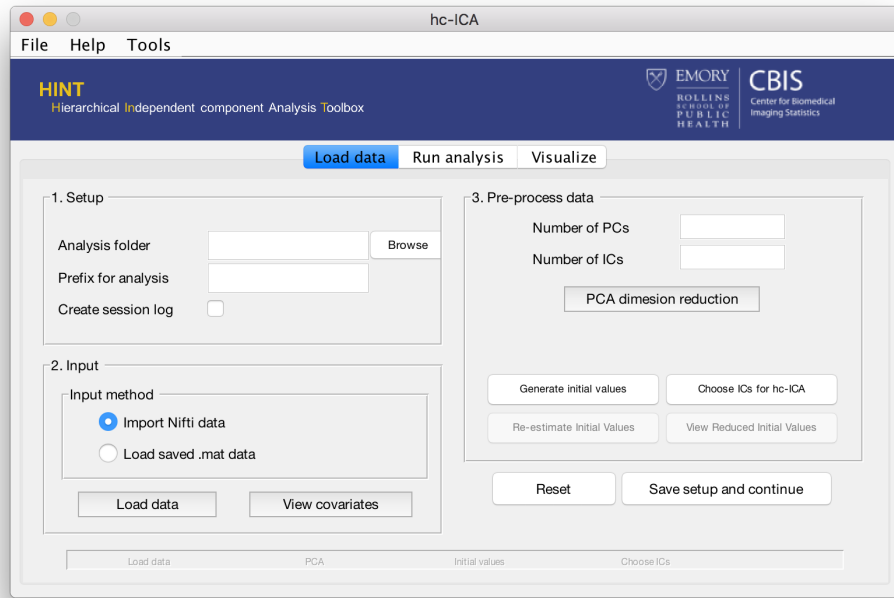


Figure 1: The preprocessing panel in which the user inputs and preprocesses the data, as well as obtains a list of ICs for analysis and initial values for the EM algorithm.

Table 1: The objects contained in the runinfo file.

Variable	Description
N	The number of subjects
X	The design matrix
YtildeStar	The $Nq \times V$ matrix of preprocessed data
beta0Star	The initial guess for the beta maps
covariates	The covariate names
covfile	The filepath to the covariate file
isCat	A $p \times 1$ vector indexing categorical covariates
maskfl	The path to the mask file
niifiles	A cell array of paths to the subject level fMRI data
numPCA	The number of principal components for preprocessing
outfolder	Path to the output directory
prefix	Prefix for the files in the analysis
q	The number of independent components
thetaStar	Structure containing initial guess values
time_num	The number of time points for each subject
voxSize	The dimension of the mask

Table 2: An example covariate file structure.

subject	age	group	race
subject1	45	trt	1
subject2	38	ctrl	2
⋮	⋮	⋮	⋮
subject20	67	trt	2

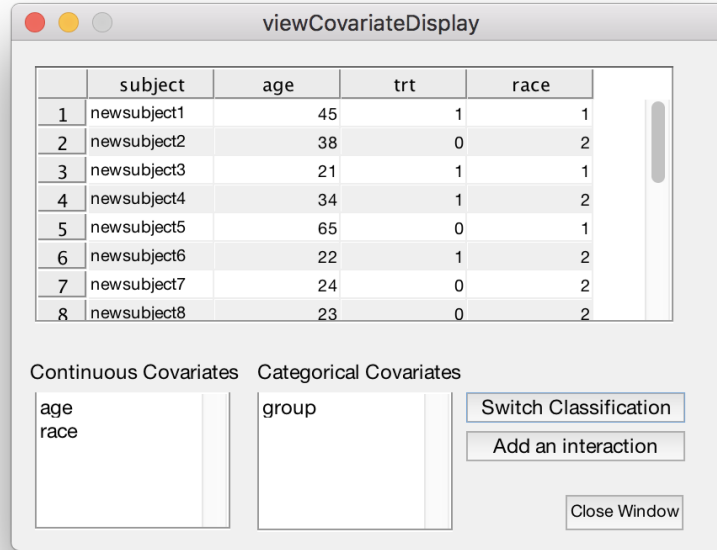


Figure 2: The covariate display window. Here the user can verify that covariates were coded correctly and add interaction effects.

file followed by each of the covariate settings for that subject. An example covariate file layout is provided in Table 2.

After reading in the data, the user has the option to “View covariates” to confirm that the data was coded correctly. By default, the HINT will treat string variables (e.g. group) as categorical variables and perform reference cell coding using the level in the first data row as the baseline. On the other hand, numeric variables will be treated as continuous covariates (e.g. age). If the user wishes to use integer codings for categorical covariates (e.g. race), they can specify this using the “View covariates” window shown in Figure 2. Additionally, this window can be used to specify any interactions of interest.

3.1.3 Initial Parameter Guesses

Under the HINT framework, an EM algorithm is used to obtain parameter estimates for the hierarchical models. These algorithms require a set of initial guesses to work. While it is possible to use a random start, it is much more accurate and efficient to select an initial guess that is as

close to the true parameter values as possible. Thus, we use a standard group ICA method to obtain initial guesses for the EM algorithm and then use our algorithm to refine the parameter estimates for the hierarchical models.

The HINT obtains initial parameter estimates for the EM algorithm using the Group ICA Of fMRI Toolbox (GIFT) described in Calhoun et al. (2001). The GIFT estimation process consists of two stages of dimensionality reduction. First, each subject’s data is reduced to c principal components. Then, the PCA-reduced subject data is stacked to create a single $Nc \times V$ data set. Spatial ICA is then performed on this data set to obtain the $q \times V$ independent components and the corresponding mixing matrix. Back reconstruction can then be performed as described in Calhoun et al. (2001) to obtain subject-specific ICs. Once the final set of ICs has been selected, initial guesses for the EM algorithm are obtained as follows:

Subject Level ICs The back-reconstructed subject level ICs from GIFT are used as the initial guess for the subject level ICs, \mathbf{s}_i .

Covariate effects and baseline ICs We use dual regression to obtain initial estimates for the β and \mathbf{s}_0 terms.

Random subject-level variability The initial guess for the subject level error variance is the variance of the residuals, $\gamma_i(v)$, from the above dual regression procedure.

Subject level mixing matrices The initial guess for the subject level temporal mixing matrices, \mathbf{A}_i , is the parameter estimates for the regression of the subject level ICs onto the preprocessed data \mathbf{Y}_i . Symmetric orthogonalization is then performed, as the preprocessed subject level data are prewhitened and thus the temporal mixing matrices should be orthogonal.

Subject level error The initial guess for the subject level error variance is the variance of the residuals from the above regression procedure for the mixing matrices.

Mixture Model Terms We fit a Gaussian mixture model to each of the \mathbf{s}_0 estimates. The gaussian component with the largest mean (in absolute magnitude) is taken to be the IC source signal, and its variance is taken as the estimate of σ_l^2 . The initial π guess is the probability of belonging to that component and the probability of the observed signal being noise is $1 - \pi$.

3.1.4 IC Selection

After obtaining initial guesses, the HINT provides the user with the opportunity to review the initial group level ICs via the “choose ICs” button before initiating the analysis. It is often desirable to remove one or more ICs from the analysis (Salimi-Khorshidi et al. (2014), Griffanti et al. (2014)). If the user determines that some ICs are not of interest, they can be removed from the data. We then obtain an updated initial guess using the GIFT. Removing ICs has the advantage of speeding up the computation time of the EM algorithm.

3.2 Analysis Panel

Figure 4 displays the analysis panel. Here, the user selects the maximum number of iterations and the convergence requirements for the estimation procedure. The options are:

Max Iterations The maximum number of EM algorithm iterations. Note that the results are saved at the end of each iteration, thus there is no risk in setting this to a high value (eg. 100) as the algorithm can be terminated at any time without loss of the most up-to-date estimates.

Epsilon 1 The L_2 distance termination criteria between all parameters (covariate effects excluded) at the end of the current iteration and the previous iteration, normalized by the magnitude of the estimates at the previous iteration.

Epsilon 2 The L_2 distance termination criteria between the covariate effects at the end of the current iteration and the previous iteration, normalized by the magnitude of the parameter estimates at the previous iteration. This value tends to be less stable, and thus there is more change from iteration to iteration.

After selecting “Run”, the user can track the algorithm’s progress using the two plots on the right hand side of the panel. If at some point the user is satisfied with the progress, but the termination criteria have not yet been met, the user can manually terminate the algorithm using the “Stop” button. In this case, the algorithm will terminate at the end of the current iteration.

3.3 Visualization Panel

Figure 5 displays the visualization panel in the HINT. Here the user can view the results of the performed analysis or load a previous runinfo file to view the results of that analysis. If multiple runinfo files exist in the same folder, the user will be asked to select a file based on the prefix.

While each of the display viewers is different in terms of what is displayed, there are some commonalities between windows. Specifically, there is a “Location and Crosshair Information” panel in each viewer that provides the user with spatial information obtain their selection. From this window the user can view the location of their crosshair, the corresponding Broddman area, and the value at that crosshair, which will either be the raw intensity score or the Z-score, depending on the user’s selection.

For this paper, we demonstrate the viewers using the results from two sub-populations, one consisting of meditators and the other of controls. The user can select between the four display window types described in the following four sub-sections. While all four panels can be accessed from the visualization panel, they can also be accessed from the “File” dropdown menu within each viewer.

Whole Group-Level Display

The first display window, the group level display, allows the user to view the population-level average maps. These correspond to the average \mathbf{s}_i for subjects $i = 1, \dots, N$. An example of the group level display window is provided in Figure 6. This panel allows for a general view of the spatial form of each IC, regardless of covariate pattern. It also provides some additional functionality. For example, from this window, the user can threshold the images either manually using the threshold box, or via a slider. Thresholded masks can then be created based on these images, which can then be applied in other display windows such as the single-subject window.

Sub-population Display

This window allows the user to specify and view IC maps for different sub-populations. For a sub-population described by a user-defined combination of covariate values \mathbf{x} , the window will display the estimated sub-population map:

$$\hat{\mathbf{s}} = \hat{\mathbf{s}}_0 + \mathbf{x}^T \hat{\boldsymbol{\beta}}$$

When running hc-ICA on multiple groups of interest, an investigator will likely be interested in how specific sub-populations differ. Through this window, the investigator can specify covariate patterns for sub-populations of interest and compare them using the comparison window (Figure 7). This window allows side-by-side viewing and thresholding of sub-population maps.

Sub-Subject Display

The single-subject viewer allows an investigator to view the estimated spatial maps for each subject in the study. These maps can be viewed much in the same way as group maps. It is also possible to apply the user-created masks from the group-viewer to these images, allowing the investigator to see how well the individual subjects conform to the group level results. See Figure 8 for an example of this window.

Beta Coefficient Display

It is likely that one of the primary questions of interest for any investigator is how the covariate patterns affect the spatial maps. In the HINT framework, this effect is captured by the beta-coefficient maps, which reflect the change from baseline captured by the covariate (β in Model 3). This final display window allows the user to view these maps overlaid on the brain.

The user can use this window to view the specific beta maps for a single covariate or specify linear combinations of the covariates. Inference can then be performed using the procedure described in Section 2.4.

4 Summary

In this paper we introduced the HINT framework implementing hierarchical ICA. While this paper focused on the implementation of the hc-ICA model in the toolbox, other methods such as a longitudinal hc-ICA are being developed. Future work will implement add techniques to the toolbox.

5 Acknowledgements

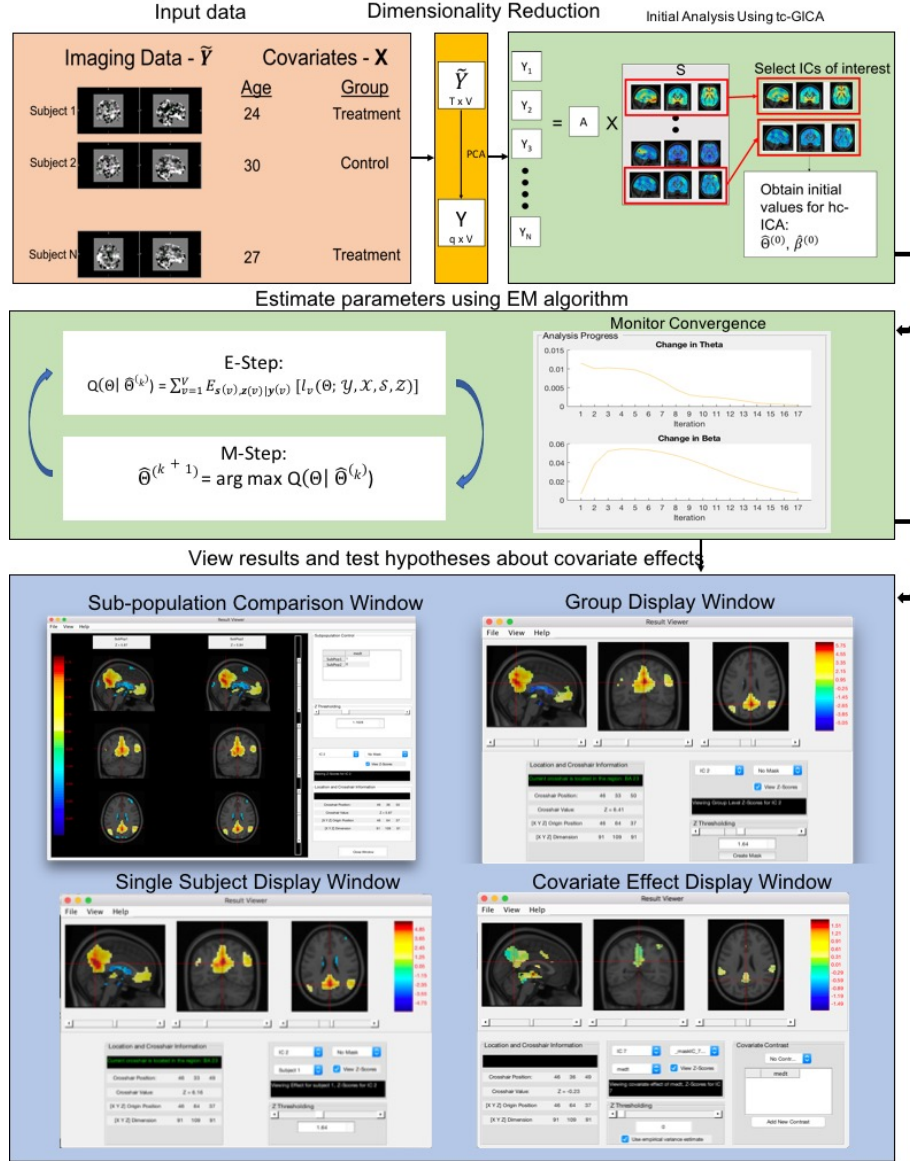
Research reported in this publication was supported by the National Institute Of Mental Health of the National Institutes of Health under Award Number ROI MH105561 and R01MH079448. The content is solely the responsibility of the authors and does not necessarily represent the official views of the National Institutes of Health.

References

- Beckmann, C. F., DeLuca, M., Devlin, J. T., and Smith, S. M. (2005). Investigations into resting-state connectivity using independent component analysis. *Philosophical Transactions of the Royal Society of London B: Biological Sciences*, 360(1457):1001–1013.
- Beckmann, C. F., Mackay, C. E., Filippini, N., and Smith, S. M. (2009). Group comparison of resting-state fmri data using multi-subject ica and dual regression. *Neuroimage*, 47(Suppl 1):S148.
- Beckmann, C. F. and Smith, S. M. (2004). Probabilistic independent component analysis for functional magnetic resonance imaging. *IEEE transactions on medical imaging*, 23(2):137–152.
- Biswal, B. B. and Ulmer, J. L. (1999). Blind source separation of multiple signal sources of fmri data sets using independent component analysis. *Journal of computer assisted tomography*, 23(2):265–271.
- Calhoun, V., Adali, T., Pearlson, G., and Pekar, J. (2001). A method for making group inferences using independent component analysis of functional mri data: Exploring the visual system. *Neuroimage*, 13(6):88.

- Daubechies, I., Roussos, E., Takerkart, S., Benharrosh, M., Golden, C., D’ardenne, K., Richter, W., Cohen, J., and Haxby, J. (2009). Independent component analysis for brain fmri does not select for independence. *Proceedings of the National Academy of Sciences*, 106(26):10415–10422.
- Griffanti, L., Salimi-Khorshidi, G., Beckmann, C. F., Auerbach, E. J., Douaud, G., Sexton, C. E., Zsoldos, E., Ebmeier, K. P., Filippini, N., Mackay, C. E., et al. (2014). Ica-based artefact removal and accelerated fmri acquisition for improved resting state network imaging. *Neuroimage*, 95:232–247.
- Guo, Y. (2011). A general probabilistic model for group independent component analysis and its estimation methods. *Biometrics*, 67(4):1532–1542.
- Guo, Y. and Pagnoni, G. (2008). A unified framework for group independent component analysis for multi-subject fmri data. *NeuroImage*, 42(3):1078–1093.
- Guo, Y. and Tang, L. (2013). A hierarchical model for probabilistic independent component analysis of multi-subject fmri studies. *Biometrics*, 69(4):970–981.
- Hyvärinen, A. and Oja, E. (2000). Independent component analysis: algorithms and applications. *Neural networks*, 13(4):411–430.
- McKeown, M. J., Makeig, S., Brown, G. G., Jung, T.-P., Kindermann, S. S., Bell, A. J., and Sejnowski, T. J. (1997). Analysis of fmri data by blind separation into independent spatial components. Technical report, NAVAL HEALTH RESEARCH CENTER SAN DIEGO CA.
- McLachlan, G. and Peel, D. (2004). *Finite mixture models*. John Wiley & Sons.
- Minka, T. P. (2001). Automatic choice of dimensionality for pca. In *Advances in neural information processing systems*, pages 598–604.
- Salimi-Khorshidi, G., Douaud, G., Beckmann, C. F., Glasser, M. F., Griffanti, L., and Smith, S. M. (2014). Automatic denoising of functional mri data: combining independent component analysis and hierarchical fusion of classifiers. *Neuroimage*, 90:449–468.
- Shi, R. and Guo, Y. (2016). Investigating differences in brain functional networks using hierarchical covariate-adjusted independent component analysis. *The annals of applied statistics*, 10(4):1930.
- Smith, S. M., Beckmann, C. F., Andersson, J., Auerbach, E. J., Bijsterbosch, J., Douaud, G., Duff, E., Feinberg, D. A., Griffanti, L., Harms, M. P., et al. (2013). Resting-state fmri in the human connectome project. *Neuroimage*, 80:144–168.
- Smith, S. M., Miller, K. L., Moeller, S., Xu, J., Auerbach, E. J., Woolrich, M. W., Beckmann, C. F., Jenkinson, M., Andersson, J., Glasser, M. F., et al. (2012). Temporally-independent functional modes of spontaneous brain activity. *Proceedings of the National Academy of Sciences*, 109(8):3131–3136.
- Tursa, J. (2011). Mtimesx - fast matrix multiply with multi-dimensional support. <https://www.mathworks.com/matlabcentral/fileexchange/25977-mtimesx-fast-matrix-multiply-with-multi-dimensional-support>.

Figure 3: The workflow within the HINT.



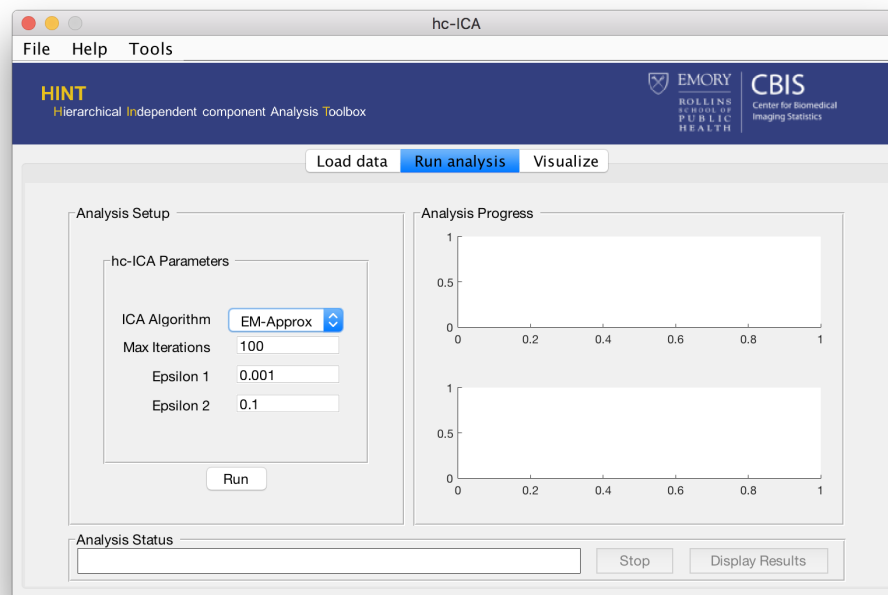


Figure 4: The HINT analysis panel. This panel allows the user to select settings for the estimation procedure and to track the progress of the algorithm via change plots.

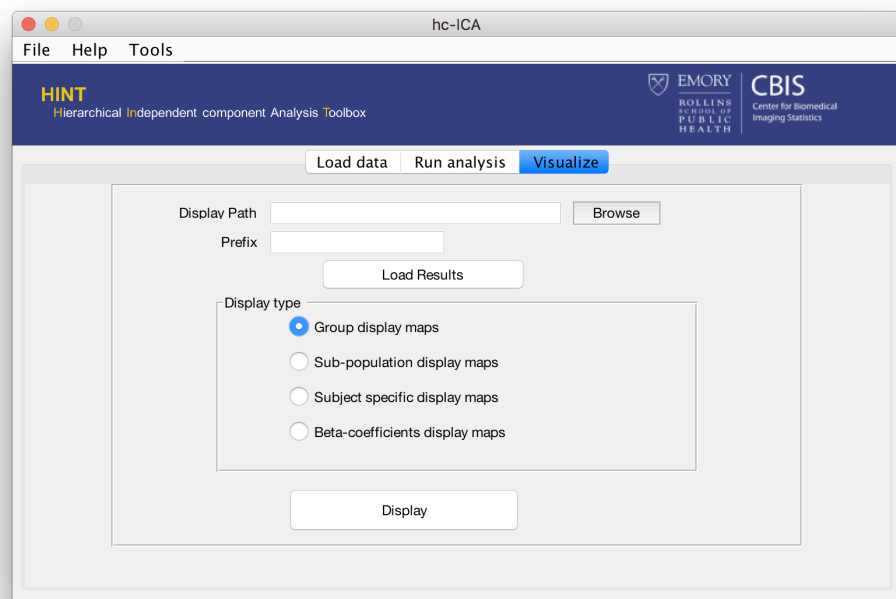


Figure 5: The HINT visualization panel. In this panel the user can view the overall group-averaged maps, compare sub-populations, look at the estimated ICs for individual subjects, and examine the estimated beta coefficient maps.



Figure 6: The HINT group-level display window. Here the user can view the population average maps, as well as create masks using the “create mask” button in the lower right-hand panel. These masks can be applied in other windows such as the single subject viewer.



Figure 7: Demonstration of the sub-population comparison window. Sub-populations based on user-defined covariate patterns can be generated and viewed using this display window. The subpopulation control box in the upper-right hand corner allows the user to view the corresponding covariate values.



Figure 8: The HINT single-subject viewer. The user can select the estimated maps for each individual subject as well as apply masks generated using the whole-group viewer.